Reactive Thread Spray Mass Spectrometry for Localization of C=C Bonds in Free Fatty Acids: Applications for Obesity Diagnosis

Devin J. Swiner, Dmytro S. Kulyk, Hannah Osae, George R. Durisek III, and Abraham K. Badu-Tawiah*

Department of Chemistry and Biochemistry, The Ohio State University, Columbus, OH 43210, United States.

ABSTRACT: Cellulose thread substrates offer a platform for microsampling and reactive ionization of free fatty acid (FFA) isomers for direct differentiation by mass spectrometry. Ambient corona discharge forms when direct current high voltage is applied to the tiny sub-fibers on the thread substrate in the presence of a polar spray solvent (MeOH/H_2O, 2:1, v/v) facilitating chemical reactions across C=C bond of unsaturated fatty acids. The process was applied for diagnosis of obesity, which we observed to show a better discriminatory power when compared with determinations based on body mass index. Overall, the integrated reactive thread-based platform is capable of (i) microsampling and dry-state, room temperature storage (>30 days) of the biofluids, (ii) in-capillary liquid/liquid extraction, and (iii) *in-situ* epoxidation reactions to locate C=C bond position in unsaturated fatty acids *via* reactions with reactive oxygen species present in ambient corona discharge. The study showcased the ability to correctly characterize FFAs, including degree of unsaturation, and the determination of their relative concentrations in clinical biofluid samples.

INTRODUCTION

Obesity can serve as a risk factor for many chronic conditions and diseases.[1,2] It is also a criterion for metabolic syndrome,[3,4] which describes a cluster of factors (e.g., high blood pressure, high triglyceride levels, high glucose levels, etc.) that lead to an increased risk of these diseases. Common obesity-related conditions are Type 2 diabetes and cardiovascular disease.[5] In 2019, heart disease was reported to be a leading killer in the United States, increasing especially in older (>65 years old) populations.[6] Understanding body metabolism and pathogenesis of these diseases remains important clinically to help establish proper prevention and treatment protocols.

Body mass index based on height and weight is typically used to measure *body* fat.[7] Unfortunately, this diagnostic strategy cannot express fat deposition in the body. Screening for early signs of obesity will require chemical tools that can quantify fat deposits. Body fat, or lipids, breaks down to form high concentrations of free fatty acids (FFAs) in serum and plasma.[8,9] Fatty acid metabolism, in turn, has been used to monitor the progression of various diseases.[10,11] In general, there are different fatty acid compositions for healthy and diseased state biological samples and those differences can be identified with many analytical techniques, such as nuclear magnetic resonance (NMR),[12,13] liquid chromatography-mass spectrometry (LC-MS)[14–16] and gas chromatography- mass spectrometry (GC-MS).[17–19] While these traditional methods are sensitive and selective, they require extensive sample preparation and large amounts of solvent and sample.

Aside from pre-analytical challenges, these nonpolar FFAs are structurally diverse, existing biologically with their isomers, making their characterization and differentiation important. Traditionally, standalone mass spectrometry is silent to molecular isomers, since the mass-to-charge (*m/z*) ratio of a given set of isomers is the same. Mitigating this problem typically includes the use of a separation technique, like LC, GC, or ion mobility, that can separate the isomers before MS detection in two distinct steps. To circumvent this analytical challenge, related to the differentiation of positional isomers of FFAs (i.e., fatty acids that differ only in double bond positions)[20,21], we propose that an integrated analytical system capable of microsampling of biofluid (<50 μL), direct analysis of collected samples, and *in-situ* reactions specifically at the C=C position during MS analysis will serve to improve the utility of standalone mass spectrometers in clinical applications without sophisticated front-end sample processing. Such capability will be useful for field, point-of-care analysis using portable mass spectrometers especially in resource-limited settings.

Herein, we present a reactive thread spray MS platform that enables ambient ionization of FFAs directly from untreated biofluids (e.g., serum and plasma) while also facilitating epoxidation reactions across C=C bonds via an atmospheric pressure chemical ionization (APCI) mechanism. When wetted by a suitable solvent (e.g., methanol/water, 2:1, vol./vol), the tiny sub-fibers in cellulose thread substrate allow the generation of ambient corona discharge upon the application of –4 kV direct current (DC) high voltage. The discharge results from the presence of the high electric field generated at the tip of the sub-micron thread fibers. The presence of water, ambient air, and energetic electrons in the vicinity where the corona discharge is generated initiates plasma reactions (in the form of APCI)[22,23] that result in the formation of reactive oxygen species such as ozone (O_3), atomic oxygen (O), and singlet oxygen ($^1O_2$). The oxidizing abilities of these reactive oxygen species are well known, including the ability of atomic oxygen to oxidize C=C double bond(s)[24] to form an epoxide (M+O). The epoxide product ions $[M+O–H]^-$ are known to undergo unique fragmentation[25,26] when subjected to collisional activation in tandem MS (MS/MS) to give a set of diagnostic ions that are specific to the number and position of the double bonds in FFAs.

Recently, several analytical platforms have been reported that focus on C=C localization.[27,28] These can be categorized into two distinct groups: 1) gas-phase reactions utilizing energetic photons in photodissociation[29] or ozone reagents in ozonolysis[30,31] under the high vacuum environment of the mass spectrometer and 2) condensed-phase chemical reactions occurring at atmospheric pressure involving external reagents such as acetone for online Paternò-Büchi photochemical reactions, dioxirane for offline solution/LTP (low-temperature plasma) interfacial reactions, *meta*-chloroperoxybenzoic acid for bulk-phase epoxidation reaction,[32,33] hydrochloric acid for online reactions[34] in nano-electrospray ionization (nESI) utilizing glass capillaries with large orifices, and NH_4OH for online epoxidation in traditional nESI that employs reactive electrodes such as Ir.[27] The current work joins a third category in that it seeks to develop a self-sustained analytical system that harnesses the electrical energy from electrospray to induce chemical reactions under ambient conditions and in real-time during ionization without the use of external reagents or plasma gases.[35–37] The following four additional attributes can be identified in favour of our reactive thread spray methodology: i) simplicity, requiring no modification of existing instrumentation, ii) low-cost, as the device is created from spooled cellulose thread substrates, iii) the ability to analyze complex mixtures directly without any sample workup, and iv) high sensitivity due to a delayed extraction mechanism that cannot not be implemented in any other substrate-based ambient ionization method such as paper spray,[38] coated blade spray,[39] and touch spray.[40]

Our previous studies on thread spray[41–44] all focused on non-reactive spray conditions. This is our first report focusing on implementation of an APCI-based mechanism in thread spray. We aimed to apply the optimized reactive thread spray MS platform to detect FFA concentrations in serum and to localize the C=C bond positions in different FFA taken from obese and healthy patients. We are interested in studying how the relative concentrations of oleic (18:1, omega-9), cis-vaccenic (18:1, omega-7), linoleic (18:2, omega-6), α-linolenic (18:3, omega-3), γ-linolenic (18:3, omega-6), palmitic (16:0), and stearic (18:0) acids vary from both sets of samples (**Figure 1**). Given that the saturated fatty acids (palmitic acid and stearic acid) have no unique fragmentation patterns

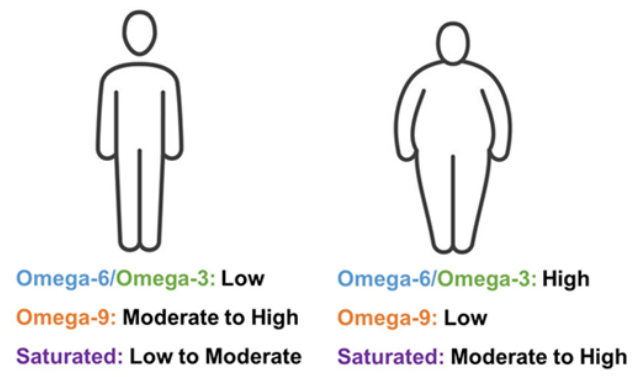

Figure 1. General overview of fatty acid type and concentration for clinically healthy and obese patients.

in the non-polar alkyl chain, (except for the loss of water, CO, and CO2 from the carboxylic headgroup), characterization studies focused on the unsaturated analytes via their epoxide reaction products using reactive thread spray. As will be shown, the reactive thread MS platform enabled standalone MS, that are traditionally silent to isomeric species, to differentiate these isobaric fatty acid analytes in untreated clinical samples.

EXPERIMENTAL SECTION

Chemicals and Reagents. Oleic acid (analytical standard) was purchased from Supelco (Bellefonte, PA). Palmitic acid (≥ 99%), stearic acid (Grade 1, ≥ 98.5%, capillary GC), palmitoleic acid (98.5%, GC), cis-vaccenic acid (≥ 97%, capillary GC), linoleic acid (≥ 99%), linolenic acid (≥ 99%), and γ-linolenic acid (≥ 99%), and methanol (99.9%, HPLC grade) were purchased from Sigma-Aldrich (St. Louis, MO). 100% 18.2 MΩ water was obtained from a Milli-Q water purification system (Millipore, Billerica, MA). 100% Cotton spool thread was purchased from a local store (JoAnn Fabrics, Columbus, OH) and Kimble 51 expansion borosilicate glass melting point capillaries (O.D. 1.5 mm) were purchased from Kimble Chase (Rockwood, TN). Human serum samples were purchased from Innovative Research (Novi, MI).

Mass Spectrometry. Mass spectra were acquired on a Thermo Fisher Scientific Finnigan LTQ linear ion trap mass spectrometer (San Jose, CA, U.S.A.). The tip of the thread (length= 50-60 mm) was positioned parallel to the MS inlet via a copper alligator clip, which was connected to an external high-voltage supply (0-6 kV). The thread spray ionization method generates ions without gas assistance so a close interface distance (0.5-5 mm) between the tip and the MS inlet was used to optimize signal intensity. MS parameters used were as follows: 200 °C capillary temperature, 3 microscans, and 60% S-lens voltage. Ion transfer optics were not optimized outside of S-lens voltage. Thermo Fisher Scientific Xcalibur 2.2 SP1 software was applied for MS data collecting and processing. Tandem MS with collision-induced dissociation (CID) was utilized for analyte identification with energies between 25-35, that was optimized for each analyte. The total run time for each of the replicates (N=5, serum volume of 10 µL) was 5 minutes, allowing for 30 second total scan time for each fatty acid.

RESULTS AND DISCUSSION

Method Optimization and Fatty Acid Characterization. To begin these studies, we used a monounsaturated fatty acid (MUFA), oleic acid (18:1, 9Z), to investigate the effect of corona discharge in thread spray and the possible epoxidation reactions. Oleic acid is classified as a non-essential omega-9 fatty acid, meaning that it can be produced in the body and supplemented in diet. MUFAs are beneficial to health and are suggested to help reduce inflammation.[45,46] In a typical experiment, a single thread, on which the sample is deposited, is placed in a glass capillary and the application of –4 kV and the polar methanol/water spray solvent yields corona discharge (**Figure 2** and **Video S1**), which produces mass spectrum that is markedly different from similar thread spray experiment conducted with non-polar ethyl acetate spray solvent (**Figure S1**). Given the reactivity of species present in a corona discharge event, this setup enables the detection of analytes of low polarity,[47,48] specifically unsaturated fatty acids, which are oxidized *via* the addition of atomic oxygen across the C=C bond. Upon collision-induced dissociation (CID) in MS/MS analysis, the epoxide reaction product dissociates to give diagnostic fragment ions. In order to form a stable corona discharge for quantitative MS analysis, solvent optimization experiments were conducted by monitoring the intensity of the expected[28] fragments for oleic acid (18:1, 9Z, omega-9) at *m/z* 155 and 171 (**Figure 3A**). We found methanol: water, 2:1 (vol./vol.) solution to be the optimal spray solvent (**Figure S2A**). Note that FAs having the same double bond position (e.g., oleic acid, 18:1, 9Z and palmitoleic acid, 16:1, 9Z) produce the same diagnostic ions when subjected to CID. However, palmitoleic acid (MW 254 Da), an omega-7 MUFA, can be

differentiated from oleic acid (omega-9; MW 282 Da) using molecular weight information. Thus, MS/MS experiments at *m/z* 269 target the epoxide product from palmitoleic acid to give diagnostic ions at *m/z* 155 and 171 (**Figure S2B and C**), which indicate double position at the 9Z position. The method is equally applicable for the differentiation of positional isomers such as oleic acid and cis-vaccenic acid (omega-7, 18:1, 11Z). While oleic acid yields *m/z* 155/171 diagnostic ion pairs, the epoxide (*m/z* 297) from vaccenic acid produces *m/z* 183 and 199 ions (**Figure S3**). The unique fragment ions from these two isomeric species mean that a mixture containing the two isomers can be analyzed effectively and directly without prior separation steps as illustrated in **Figure 3B** where 1:1 mole ratio of pure oleic and cis-vaccenic acid were mixed and subjected to reactive thread spray MS analysis.

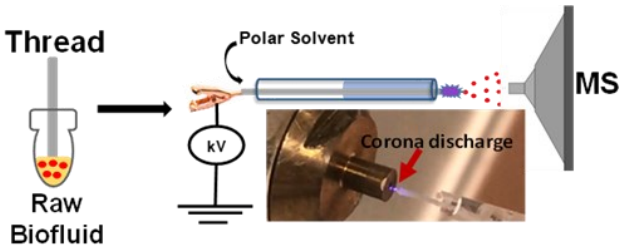

Figure 2. Schematic illustrating microsampling with cellulose thread followed by reactive thread spray MS analysis of collected biofluid via an APCI mechanism. Insert shows photograph of thread spray MS at the onset of corona discharge.

When it comes to diet, monitoring the ratio of omega-6 to omega-3 fatty acids is common.[47,48] High levels of omega-6 FAs and/or low levels of omega-3 FAs have been associated with the pathogenesis of many conditions and diseases.[49,50] The most common of the omega-6 essential fatty acids is linoleic acid (18:2, MW 280 Da), which can only be obtained through diet. One of the metabolic pathways of linoleic acid include its conversion to arachidonic acid (20:4, MW 304 Da) potentially leading to pro-inflammatory responses in the body.[51,52] Conversely, the most common omega-3 essential fatty acid is α-linolenic acid (18:3, MW 278 Da). α-Linolenic acid is a precursor for eicosapentaenoic acid (20:5, MW 302 Da) and docosahexaenoic acid (22:6, MW 328 Da). These long chain FAs are responsible for anti-inflammatory activity in the body[53] and can be useful in reducing the risk of obesity-related diseases.[54,55] The overall goal for health and diet is to balance the intake of these classes of FAs. Therefore, ability to monitor the relative concentrations of these polyunsaturated fatty acids (PUFAs) directly from biofluids can be very useful, which we demonstrate using the reactive thread spray MS platform.

Encouraged by results from the analysis of MUFAs, we applied the optimized parameters of the reactive thread spray MS method (spray voltage and solvent composition) for the characterization of linoleic (18:2, 9Z and 12Z) and isomers α-linolenic (18:3, 9Z, 12Z, and 15Z) and γ-linolenic (18:3, 6Z, 9Z, and 12Z) polyunsaturated fatty acids (**Figure S4B and C**). For example, linoleic acid has double bonds in the 9Z and 12Z positions, which can both undergo oxidation. For a non-selective epoxidation reaction, we expected mono-epoxide product to compose of a mixture consisting of reaction at both double bond positions. Therefore, the isolation of $[M+O-H]^-$ at *m/z* 295 in MS/MS experiments followed by activation upon CID should yield a mixture of four diagnostic fragment ions corresponding to two pairs of ions for the respective double bond positions (**Figure S4A**). **Table 1** summarizes the diagnostic ion pairs for all fatty acids tested in this study. It is important to note that these three PUFAs are not the only highly abundant FAs of this class. The purpose of this study was to begin exploring the capabilities of reactive thread spray. Future studies will be more comprehensive and explore longer chained PUFAs.

Profiling of Clinically Obese Samples by Reactive Thread Spray MS. The ability to collect microvolumes of biofluid samples in the cellulose thread substrate and to perform direct analysis can be enormously beneficial for personalized healthcare. This is because such an advanced healthcare system requires sample collection away from the laboratory, something that is currently challenged by our inability to preserve the microsample integrity during transport. Not only does the thread spray method enable microsampling and sample storage under ambient conditions without cold storage requirements, but it also uses ambient air to generate stable corona discharge at moderate DC voltages for *in-situ* epoxidation of C=C bonds for

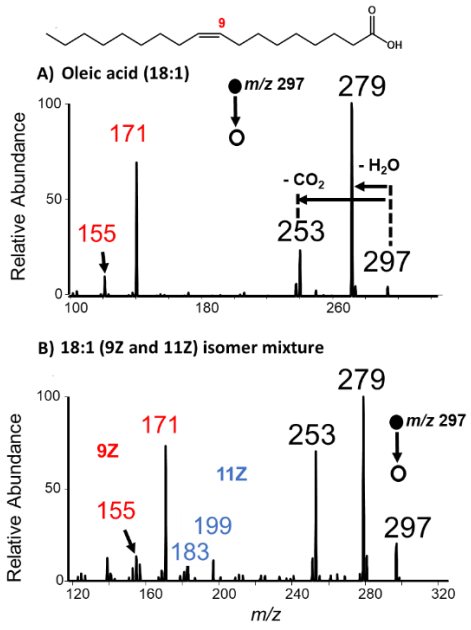

Figure 3. Tandem MS spectra of A) pure solution of oleic acid and B) 1:1 equimolar solution of oleic and cis-vaccenic acid. Solution concentrations were 200 μM in 2:1 methanol: water (vol./vol.)**.** CID energy was between 25-35 manufacturer's units.

Table 1. Summary of fatty acid analytes and their corresponding diagnostic fragment ion pairs as derived from direct analysis by reactive thread spray MS.

Acid	Omega Notation	MW (g/mol)	$[M-H]^-$	$[M+O-H]^-$	Diagnostic Fragments (m/z)
Palmitic (16:0)	-	256	255	-	211, 237
Stearic (18:0)	-	284	283	-	239, 265
Palmitoleic (16:1)	Omega-7	254	253	269	155, 171
Oleic (18:1)	Omega-9	282	281	297	155,171
Cis-vaccenic (18:1)	Omega-7	282	281	297	183,199
Linoleic (18:2)	Omega-6	280	279	295	155,171; 195,211
α-Linolenic (18:3)	Omega-3	278	277	293	155,171; 195,211; 235, 251
γ-Linolenic (18:3)	Omega-6	278	277	293	113,129; 153,169; 193, 209

subsequent differentiation of positional isomers of MUFAs and PUFAs using a standalone mass spectrometer. The unique advantage presented by this method is that this procedure can be implemented in a resource-limited setting (e.g., on a portable instrument) since no sample preparation and plasma/spray gases are required. In addition, when utilized for direct biofluid analysis, the thread spray platform offers delayed extraction and enrichment capabilities without solvent evaporation limitations. This is contrary to other substrate-based ambient ionization methods where rapid solvent evaporation in the open environment of the ion source mandates the synchronization with MS analysis during analyte extraction.[56,57] The inevitable consequence is limited sensitivity due to inefficient analyte extraction (occurring on time scales of fraction of seconds) during the synchronized analysis. Thread spray offers an optimized 60 s delayed extraction capabilities for enhanced sensitivity.[41]

It is important to note that the thread spray ion source is made reactive only when using highly polar spray solvents in the negative-ion mode. The reactivity can be turned off simply by changing spray solvent (**Figure S5**). We applied the reactive thread spray strategy developed in this work to characterize clinically obese serum samples. In this proof-of-concept study, we selected samples from two donors (Obese 1 and Obese 2) who had no history of smoking, medication use, and pre-existing conditions (**Table S1**). This allows us to control potential interferences of these factors with free fatty acid serum concentrations. The two obese samples were characterized in terms of total cholesterol, triglyceride concentration, high-density lipoprotein (HDL), and low-density lipoprotein (LDL) levels. Lipemia levels of the samples were characterized as medium and low for Obese 1 and Obese 2, respectively, by Innovative Research. We used the reactive thread spray MS method to gain insight in discerning whether the two samples can be distinguished based on their free fatty acid composition and relative concentration.

To do this, we analyzed a total of eight (8) FFAs, six of which were unsaturated and two saturated. Fatty acid profiles were created using five replicate serum samples. Obese 1 and Obese 2 samples were used to create a baseline to showcase how FA profiles can vary for different levels of obesity. We also spiked a separate non-obese serum sample with 200 μM concentrations of each fatty acid to serve as a control. Moreover, we used two additional serum samples as blind samples in which their obesity status and chemical composition were unknown. That is, no clinical data was provided for these blind samples. This targeted profiling study was achieved via the use tandem MS for the selected eight free FAs. MS/MS product ion intensities were used to determine the relative amounts of omega-3, -6, and -9 FAs to make inferences about the diets of the four patients used in this study (i.e., two obese and two blind samples). In general, patients with metabolic syndrome are expected to have higher omega-6 and lower omega-9 content[52] relative to control samples. These same people would also have high saturated FFA content, which is associated with excessive intake of butters, sugars, and starches, that have been shown to increase the risk for obesity-related diseases by increasing plaque build-up in the arteries.[58,59] Therefore, in addition to the common unsaturated FAs, we also monitored two of the most common saturated FAs found in meats, cheeses, and dairy products, palmitic (16:0) and stearic (18:0) acids. While these FAs have no double bonds to undergo oxidation, we used their respective fragments denoting the losses of H_2O and CO_2 to confirm their presence in these studies.

Experiments were conducted as described above where a single thread was dipped into 10 μL of serum and then placed inside a glass capillary for proper application of solvent and voltage for MS detection. **Figure 4** shows FA profiles of the spiked control, Obese 1, and Obese 2 samples. These profiles were constructed to aid data visualization and to show relative amounts of each fatty acid in comparison to each other. This is, the eight FAs chosen are not fully inclusive of those that are relevant clinically. The spiked serum profile (**Figure 4A**) shows relative ionization efficiencies for the equimolar mixture of the eight fatty acids. Hydrophobic analytes are known to have higher ionization efficiencies,[60] and we see a similar correlation with our

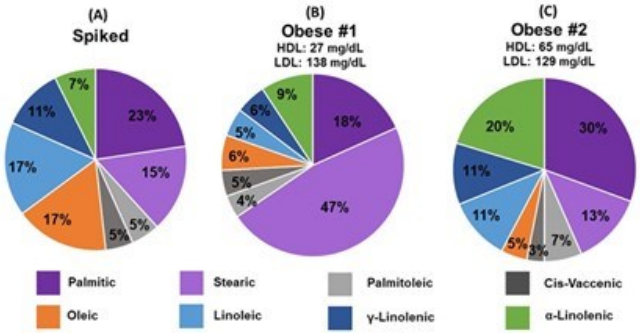

Figure 4. Free fatty acid profiles for (A) control, spiked serum sample, (B) Obese 1 serum sample and (C) Obese 2 serum sample. Each percentage provided is relative to the total intensity of the eight fatty acids analyzed in the sample. The different shades of a given color are representative of different fatty acids of the same class. Purple = saturated, grey = omega-7, orange = omega-9, blue = omega-6, and green = omega-3.

method. For example, based on log P values,[61] the saturated fatty acids have higher log P values (palmitic acid, log P =7.17 and stearic acid, log P = 8.23) than the unsaturated acids (linoleic acid, log P = 7.05 and α-linolenic acid, log P = 6.64), which is reflected in **Figure 4A**. The magnitude of and other factors related to (e.g., double bond position or degree of oxidation, etc.) the differences in ionization efficiencies of these analytes was not directly studied in current work but could be explored to fully understand the mechanism of APCI on thread substrates. In the current study, we used the "spiked" control serum sample to ensure that differences in fatty acid ion intensities from obesity samples are not merely due to ionization suppression. For example, this control study showed that when analyzed in equimolar concentrations, palmitic acid gives a higher ion intensity than steric acid, as well as oleic acid and α-linoleic acid.

Considering the Obese 1 profile (**Figure 4B**), it is apparent this patient has high saturated FA levels with an omega-6/omega-3 ratio of 1.12 ± 0.18. Obese 2 (**Figure 4C**) has a slightly lower saturated FA makeup with a similar omega-6/omega-3 ratio (1.08 ± 0.078). The higher content of steric acid for Obese 1 sample cannot be attributed to just ionization efficiency differences due to the fact the controlled spiked experiments revealed palmitic acid to be more easily ionized than stearic acid. Likewise, relatively high content of α-linoleic acid detected in Obese 2 sample is real when compared with Obese 1 and spiked samples. We expected to see these types of profiles for the two obese sample due to their reported low-density lipoprotein levels, which are outside of the normal range (≤ 100 mg/dL). This is addition to Obese 1 sample reported to have high-density lipoprotein levels below the normal range of ≥ 60 mg/dL.[62,63] The content of omega-9 (i.e., oleic acid) FA serves as complementary evidence for characterizing these two samples as obese. Both samples have ~5% relative concentration of omega-9 in serum compared to the eight FAs analyzed, implying that their

diets do not include large amounts of vegetable-based oils, like olive oil where oleic acid content is high.[64]

To validate the discriminatory power of our thread-based sampling and analysis platform, we analyzed two blind serum samples, Blind samples #1 and #2. We used the reactive thread spray MS method to create FFA profiles (**Figure 5**) for both blind samples. Although there is no clinical data for these blinded samples, we were able to use their FFAs profiles to make some general conclusions about their lifestyles when compared with the two obese samples previously analyzed with the same method. Blind sample #1 showed the lowest omega-6/omega-3 ratio (0.67 ± 0.075) with the lowest saturated FA makeup. Blind sample #2 on the other hand was shown to have the highest saturated FFA content and highest omega-6/omega-3 ratio (3.22 ± 0.40) of all the serum samples analyzed.

Overall, Blind sample #1 shows the most promise of a person supplementing their diet with healthier foods. For clinically healthy people, it was hypothesized that the omega-6/omega-3 ratio would be low as well as the saturated FA levels, which is seen here for Blind #1 and summarized in **Figure 6**. The sketches presented in **Figure 6B** are relative interpretations based solely on tandem MS data and the FFA profiles we obtained. For example, based on the Blind #2 profile, we can infer that their diet was lacking in proper nutrients and could mean that they have an increased waist circumference as shown in the sketch. In contrast, the profile Obese #2 suggest they had a diet more balanced than Obese 1, shown by the omega-6/omega-3 ratio, but not as balanced as Blind #1. This would mean they could be slightly overweight. We also can confirm this finding with the saturated/unsaturated ratios. Higher relative saturated content is indicative of an unbalanced diet.

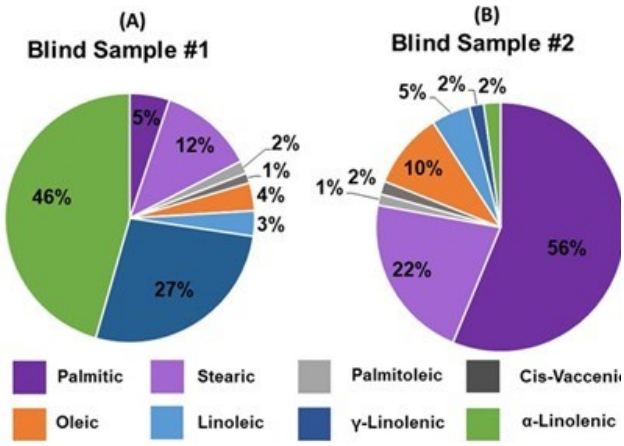

Figure 5. Free fatty acid profiles for blind serum samples. These serum samples have unknown clinical profiles. Each percentage provided is relative to the total intensity of the eight fatty acids analyzed in the sample. The different shades of a given color for both Blind #1 (A) and Blind #2 (B) samples are representative of different fatty acids of the same class. Purple = saturated, grey = omega-7, orange = omega-9, blue = omega-6, and green = omega-3.

Although body mass index (BMI) of Obese #1 (BMI = 30) is smaller than Obese #2 (BMI = 42), our FFA profile data indicate a better lifestyle/diet (or less severe form of obesity) for Obese sample #2. As suggested by others, BMI values are not a good indicator for diagnosing obesity.[65] Our data correlates well with parameters such as HDL, LDL, and triglyceride levels. Thus, we sought to use additional control samples whose HDL, LDL, and triglyceride levels we can predict to map onto high Omega-6/Omega-3 ratio. This experiment was limited by sample available, but we identified one clinical sample that matched our LDH/LDL/triglyceride predictions. We analyzed this sample using our reactive thread spray MS method and the corresponding ion intensities of the eight fatty acids were measured. The FFA profile of this experiment is provided in **Figure S6**, which closely resembled FFA profile for Blind #2 and Obese #1 as predicted based on triglyceride and LDL levels (**Table S1**). That is, we determined omega-6/omega-3 and saturated/unsaturated ratios for the additional control samples to be 1.9 ± 0.14 and 1.5 ± 0.16, respectively. See **Figure 6A** for the corresponding values for Blind #2 and Obese #1. Instead of relying on limited commercial samples, future studies would need to increase sample size alongside tightly controlled subjects in terms of diet intake,[66] exercise regimen, and health status,[67] including pregnancy.[68] Regardless, this study serves as a strong foundation for potential applications of reactive thread spray MS for clinical diagnostics using serum samples.

To investigate the quantitative ability of the reactive thread spray MS method, we constructed standard addition calibration curves to quantify the amount of oleic acid in Obese 1 sample. We monitored the linear response for the parent epoxide peak, *m/z* 297, which is specific to reactive thread spray process. Although cis-vaccenic acid is isobaric with oleic acid, it is abundant mainly in sea buckthorn oil. This makes its contribution to the quantitation on oleic acid in human serum very small. This was confirmed by tandem MS analysis.

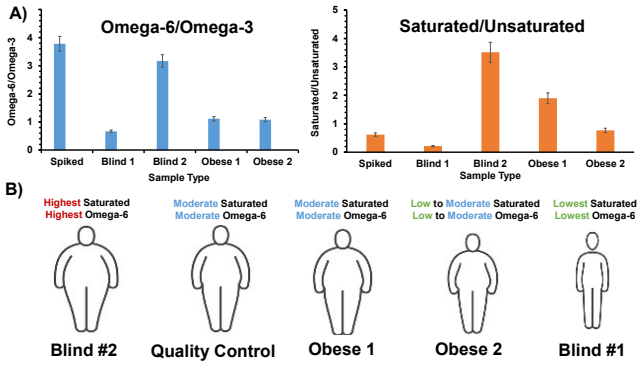

Figure 6. Data analysis for all sample types. Each fatty acid (FA) was identified by their unique fragmentation pattern, as listed in Table 1, and each class is represented by the overall sum of those fragment peaks. For example, omega-6 FAs are linoleic and γ-linolenic acids, and their fragment ion intensities were added to give an overall total "omega-6" content. Standard deviations are representative of 5 replicates. B) Suggested patient sketches based off statistical analysis and FA profiles. Note, these depictions are not confirmed since the serum samples collected and analyzed were done blind.

The unknown concentration present in Obese 1 serum was found to be 9.10 ± 0.96 µM (**Figure S7A**), which is lower than the common FFA range of 30-320 µM found in healthy serum and plasma samples[69] and thus confirming a depletion of this non-essential omega-9 fatty acid in this patient. We also monitored the unreacted oleic acid peak $[M\text{-}H]^-$ at *m/z* 281, to see if it would warrant comparable or better accuracy using this platform (**Figure S7B**). Interestingly, oleic acid concentration in this clinical sample was again found to be 10.8 ± 0.98 µM with similar precision and linearity. This proves that using the peak generated from the on-

line oxidation process for reactive thread spray is acceptable for quantification.

As already mentioned, another benefit associated with the use of thread substrate is ability to stored collected biofluid sample under ambient conditions with minimal degradation. We conducted stability tests for Obese 1 and Obese 2 serum samples focusing on three FFAs (palmitic, stearic, and oleic acids) that have shown clinical relevance (**Figure S8**). We were able to monitor the fragment peaks of these analytes and see a relatively stable signal intensity for 28 days. For both obese samples, we observed < 30% overall degradation, validating this method as one that can also be used as a storage medium prior to MS analysis for sensitive detection.

CONCLUSIONS

In conclusion, we have shown that thread spray ionization can be used in an APCI mode for the analysis of unsaturated fatty acids in serum. The reactive species generated in the corona discharge allow for on-line epoxidation reactions that can be used to differentiate between fatty acid isomers. It is also capable of discriminating between serum samples with varying levels of obesity by considering eight fatty acids and their fragmentation patterns obtained in tandem MS studies. The creation of FA profiles gives comparative data that can be used to group patient samples into classes that can potentially give insights to lifestyle and diet. The low micromolar sensitivity suggests early detection is possible with the reactive thread spray MS platform. Using three clinical controls samples, which serves as references, we were able to make inferences about blind serum samples without clinical data. We determined that relatively high omega-6/omega-3 ratios with a high saturated FA content were indicative of some level of obesity, as shown for Blind #2 and Obese 1 samples. Future studies would extend and scale up this work by increasing the sample size and conducting complementary clinical analysis, including but not limited to, dietary intake, medication, and pre-existing conditions to extend this method to obesity-related diseases such as Type 2 diabetes and cardiovascular disease.

ASSOCIATED CONTENT

The Supporting Information is available free of charge at http://pubs.acs.org.

Optimization of thread based APCI with monounsaturated fatty acids (MUFAs); MUFA isomer differentiation; polyunsaturated fatty acid (PUFA) tandem MS spectra; solvent reactivity; clinical data for obesity samples; quality control sample; standard addition curves; stability tests.

AUTHOR INFORMATION

Corresponding Author

* Prof. A.K. Badu-Tawiah − *Department of Chemistry and Biochemistry, The Ohio State University, 100 W. 18th Avenue, Columbus, OH 43210*; E-mail: badu-tawiah.1@osu.edu.

Author Contributions

The manuscript was written through contributions of all authors. All authors have given approval to the final version of the manuscript.

Notes

There are no conflicts to declare.

ACKNOWLEDGMENT

This work was supported by National Institute of Health (Award Number R01-AI-143809) and National Science Foundation (Award Number CHE-1900271).

REFERENCES

(1) Arner, P.; Rydén, M. *Obes. Facts* **2015**, *8*, 147–155.
(2) Kd, W.; D, S.; Ps, V.; Wc, W.; L, L.; St, W. *Int. J. Obes. Relat. Metab. Disord. J. Int. Assoc. Study Obes.* **1994**, *18*, 137–144.
(3) Després, J.-P.; Lemieux, I. *Nature* **2006**, *444*, 881–887.
(4) Ritchie, S. A.; Connell, J. M. C. *Nutr. Metab. Cardiovasc. Dis.* **2007**, *17*, 319–326.
(5) De Wit, N.; Derrien, M.; Bosch-Vermeulen, H.; Oosterink, E.; Keshtkar, S.; Duval, C.; de Vogel-van den Bosch, J.; Kleerebezem, M.; Müller, M.; van der Meer, R. *Am. J. Physiol.-Gastrointest. Liver Physiol.* **2012**, *303*, G589–G599.
(6) Sidney, S.; Go, A. S.; Jaffe, M. G.; Solomon, M. D.; Ambrosy, A. P.; Rana, J. S. *JAMA Cardiol.* **2019**, *4*, 1280.
(7) Nuttall, F. Q. *Nutr. Today* **2015**, *50*, 117–128.
(8) Boden, G. *Endocrinol. Metab. Clin. North Am.* **2008**, *37*, 635–646, viii–ix.
(9) Zhou, H.; Urso, C.; Jadeja, V. *J. Inflamm. Res.* **2020**, *13*, 1–14.
(10) Conquer, J. A.; Tierney, M. C.; Zecevic, J.; Bettger, W. J.; Fisher, R. H. *Lipids* **2000**, *35*, 1305–1312.
(11) Chavarro, J. E.; Stampfer, M. J.; Li, H.; Campos, H.; Kurth, T.; Ma, J. *Cancer Epidemiol. Prev. Biomark.* **2007**, *16*, 1364–1370.
(12) Brindle, J. T.; Antti, H.; Holmes, E.; Tranter, G.; Nicholson, J. K.; Bethell, H. W. L.; Clarke, S.; Schofield, P. M.; McKilligin, E.; Mosedale, D. E.; Grainger, D. J. *Nat. Med.* **2002**, *8*, 1439–1445.
(13) Tukiainen, T.; Tynkkynen, T.; Mäkinen, V.-P.; Jylänki, P.; Kangas, A.; Hokkanen, J.; Vehtari, A.; Gröhn, O.; Hallikainen, M.; Soininen, H.; Kivipelto, M.; Groop, P.-H.; Kaski, K.; Laatikainen, R.; Soininen, P.; Pirttilä, T.; Ala-Korpela, M. *Biochem. Biophys. Res. Commun.* **2008**, *375*, 356–361.
(14) Aslan, M.; Özcan, F.; Aslan, I.; Yücel, G. *Lipids Health Dis.* **2013**, *12*, 169.
(15) Nam, J.-W.; Jenkins, L. M.; Li, J.; Evans, B. S.; J. G. Jaworski, J. G.; Allen, D. K. *Plant Cell* **2020**, *32*, 820–832.
(16) Le Faouder, P.; Baillif, V.; Spreadbury, I.; Motta, J.-P.; Rousset, P.; Chêne, G.; Guigné, C.; Tercé, F.; Vanner, S.; Vergnolle, N.; Bertrand-Michel, J.; Dubourdeau, M.; Cenac, N. *J. Chromatogr. B* **2013**, *932*, 123–133.
(17) Nasaruddin, M. L.; Hölscher, C.; Kehoe, P.; Graham, S. F.; Green, B. D. *Am. J. Transl. Res.* **2016**, *8*, 154–165.
(18) Wang, D.-C.; Sun, C.-H.; Liu, L.-Y.; Sun, X.-H.; Jin, X.-W.; Song, W.-L.; Liu, X.-Q.; Wan, X.-L. *Neurobiol. Aging* **2012**, *33*, 1057–1066.
(19) Lv, W.; Yang, T. *Clin. Biochem.* **2012**, *45*, 127–133.
(20) Mahfouz, M. M.; Valicenti, A. J.; R.T. Holman, R. T. *Biochim. Biophys. Acta BBA - Lipids Lipid Metab.* **1980**, *618*, 1–12.
(21) Yang, K.; Dilthey, B. G.; Gross, R. W. *Anal. Chem.* **2013**, *85*, 9742–9750.
(22) Kulyk, D. S.; Swiner, D. J.; Sahraeian, T.; Badu-Tawiah, A. K. *Anal. Chem.* **2019**, *91* (18), 11562–11568.
(23) Kulyk, D. S.; Sahraeian, T.; Wan, Q.; Badu-Tawiah, A. K. *Anal. Chem.* **2019**, *91* (10), 6790–6799.
(24) Suga, Y.; Sekiguchi, H. *Thin Solid Films* **2006**, *506–507*, 427–431.
(25) Chintalapudi, K.; Badu-Tawiah, A. K. *Chem. Sci.* **2020**, *11*, 9891–9897.
(26) Zhao, Y.; Zhao, H.; Zhao, X.; Jia, J.; Ma, Q.; Zhang, S.; Zhang, X.; Chiba, H.; Hui, S.-P.; Ma, X. *Anal. Chem.* **2017**, *89*, 10270–10278.
(27) Song, C.; Gao, D.; Li, S.; Liu, L.; Chen, X.; Jiang, Y. *Analytica Chimica Acta* **2019**, *1086*, 82–89.
(28) Zhang, H.; Xu, M.; Shi, X.; Liu, Y.; Li, Z.; Jagodinsky, J. C.; Ma, M.; Welham, N. V.; Morris, Z. S.; Li, L. *Chem. Sci.* **2021**, *12* (23), 8115–8122.

(29) Feider, C. L.; Macias, L. A.; Brodbelt, J. S.; Eberlin, L. S. *Anal. Chem.* **2020**, *92*, 8386–8395.
(30) Paine, M. R. L.; Poad, B. L. J.; Eijkel, G. B.; Marshall, D. L.; Blanksby, S. J.; Heeren, R. M. A.; Ellis, S. R. *Angew. Chem.* **2018**, *130*, 10690–10694.
(31) Harrison, K. A.; Murphy, R. C. *Anal. Chem.* **1996**, *68*, 3224–3230.
(32) Ma, X.; Xia, Y. *Angew. Chem. Int. Ed.* **2014**, *53*, 2592–2596.
(33) Feng, Y.; Chen, B.; Yu, Q.; Li, L. *Anal. Chem.* **2019**, *91*, 1791–1795.
(34) Wan, L.; Gong, G.; Liang, H.; Huang, G. *Anal Chim Acta* **2019**, *1075*, 120–127.
(35) Takashima, S.; Toyoshi, K.; Yamamoto, T.; Shimozawa, N. *Sci Rep* **2020**, *10* (1), 12988.
(36) Zhao, X.; Zhao, Y.; Zhang, L.; Ma, X.; Zhang, S.; Zhang, X. *Anal. Chem.* **2018**, *90* (3), 2070–2078.
(37) Tang, S.; Cheng, H.; Yan, X. *Angew. Chem. Int. Ed.* **2020**, *59*, 209–214.
(38) Liu, J.; Wang, H.; Manicke, N. E.; Lin, J.-M.; Cooks, R. G.; Ouyang, Z. *Anal. Chem.* **2010**, *82*, 2463–2471.
(39) Gómez-Ríos, G. A.; Pawliszyn, J. *Angew. Chem. Int. Ed.* **2014**, *53*, 14503–14507.
(40) Kerian, K. S.; Jarmusch, A. K.; Cooks, R. G. *Analyst* **2014**, *139*, 2714–2720.
(41) Swiner, D. J.; Jackson, S.; Durisek, G. R.; Walsh, B. K.; Kouatli, Y.; Badu-Tawiah, A. K. *Anal. Chim. Acta* **2019**, *1082*, 98–105.
(42) Jackson, S.; Swiner, D. J.; Capone, P. C.; Badu-Tawiah, A. K. *Anal. Chim. Acta* **2018**, *1023*, 81–88.
(43) Swiner, D. J.; Durisek, G. R.; Osae, H.; Badu-Tawiah, A. K. *RSC Adv.* **2020**, *10*, 17045–17049.
(44) Jackson, S.; Frey, B. S.; Bates, M. N.; Swiner, D. J.; Badu-Tawiah, A. K. *The Analyst* **2020**, *145*, 5615–5623.
(45) Gonçalves-de-Albuquerque, C. F.; Medeiros-de-Moraes, I. M.; de J. Oliveira, F. M.; Burth, P.; Bozza, P. T.; Castro Faria, M. V.; Silva, A. R.; de Castro-Faria-Neto, H. C. *PLoS ONE* **2016**, *11*, DOI 10.1371/journal.pone.0153607.
(46) Gultekin, G.; Sahin, H.; Inanc, N.; Uyanik, F.; Ok, E. *Pak. J. Med. Sci.* **2014**, *30*, 299–304.
(47) Kauppila, T. J.; Kostiainen, R. *Anal. Methods* **2017**, *9*, 4936–4953.
(48) Chen, J.; Tang, F.; Guo, C.; Zhang, S.; Zhang, X. *Anal. Methods* **2017**, DOI 10.1039/C7AY00965H.
(49) Simopoulos, A. P. *Biomed. Pharmacother.* **2002**, *56*, 365–379.
(50) Simopoulos, A. P. *Biomed. Pharmacother.* **2006**, *60*, 502–507.
(51) Allayee, H.; Roth, N.; Hodis, H. N. *J. Nutr. Nutr.* **2009**, *2*, 140–148.
(52) Simopoulos, A. P. *Nutrients* **2016**, *8*, 128.
(53) Johnson, G. H.; Fritsche, K. *J. Acad. Nutr. Diet.* **2012**, *112*, 1029-1041.e15.
(54) Simopoulos, A. P. *Am. J. Clin. Nutr.* **1991**, *54*, 438–463.
(55) Swanson, D.; Block, R.; Mousa, S. A. *Adv. Nutr.* **2012**, *3*, 1–7.
(56) Frey, B. S.; Damon, D. E.; Badu-Tawiah, A. K. *Mass Spectrom. Rev.* **2019**, 1–35.
(57) Swiner, D. J.; Jackson, S.; Burris, B. J.; Badu-Tawiah, A. K. *Anal. Chem.* **2020**, *92*, 183–202.
(58) German, J. B.; Dillard, C. J. *Am. J. Clin. Nutr.* **2004**, *80*, 550–559.
(59) Group, K. S.; Rasmussen, B. M.; Vessby, B.; Uusitupa, M.; Berglund, L.; Pedersen, E.; Riccardi, G.; Rivellese, A. A.; Tapsell, L.; Hermansen, K. *Am. J. Clin. Nutr.* **2006**, *83*, 221–226.
(60) Rebane, R.; Kruve, A.; Liigand, P.; Liigand, J.; Herodes, K.; Leito, I. *Anal. Chem.* **2016**, *88*, 3435–3439.
(61) Sangster, J. *J. Phys. Chem. Ref. Data* **1989**, *18*, 1111–1229.
(62) Barter, P.; Gotto, A. M.; LaRosa, J. C.; Maroni, J.; Szarek, M.; Grundy, S. M.; Kastelein, J. J. P.; Bittner, V.; Fruchart, J.-C. *N. Engl. J. Med.* **2007**, *357*, 1301–1310.
(63) Fernandez, M. L.; Webb, D. *J. Am. Coll. Nutr.* **2008**, *27*, 1–5.
(64) Palomer, X.; Pizarro-Delgado, J.; Barroso, E.; Vázquez-Carrera, M. *Trends Endocrinol. Metab.* **2018**, *29*, 178–190.
(65) Dhurandhar, E. J. *Int. J. Obes.* **2016**, *40*, 729–730.
(66) Liu, T.-W.; Heden, T. D.; Morris, E. M.; Fritsche, K. L.; Vieira-Potter, V. J.; Thyfault, J. P. *Lipids* **2015**, *50*, 997–1008.
(67) Fernández-Real, J.-M.; Broch, M.; Vendrell, J.; Ricart, W.; *Diabetes Care* **2003**, *26*, 1362–1368.
(68) Hautero, U.; Laakso, P.; Linderborg, K.; Niinivirta, K.; Poussa, T.; Isolauri, E.; Laitinen, K. *Eur. J. Clin. Nutr.* **2013**, *67*, 1163–1168.
(69) Kish-Trier, E.; Schwarz, E. L.; Pasquali, M.; Yuzyuk, T.; *Clin. Mass Spectrom.* **2016**, *2*, 11–17.

TOC